Journal Pre-proofs

UV–VIS imaging-based investigation of API concentration fluctuation caused by the sticking behaviour of pharmaceutical powder blends

Orsolya Péterfi, Lilla Alexandra Mészáros, Bence Szabó-Szőcs, Máté Ficzere, Emese Sipos, Attila Farkas, Dorián László Galata, Zsombor Kristóf Nagy

PII: S0378-5173(24)00244-8
DOI: https://doi.org/10.1016/j.ijpharm.2024.124010
Reference: IJP 124010

To appear in: *International Journal of Pharmaceutics*

Received Date: 15 February 2024
Revised Date: 14 March 2024
Accepted Date: 14 March 2024

Please cite this article as: O. Péterfi, L. Alexandra Mészáros, B. Szabó-Szőcs, M. Ficzere, E. Sipos, A. Farkas, D. László Galata, Z. Kristóf Nagy, UV–VIS imaging-based investigation of API concentration fluctuation caused by the sticking behaviour of pharmaceutical powder blends, *International Journal of Pharmaceutics* (2024), doi: https://doi.org/10.1016/j.ijpharm.2024.124010

UV-VIS imaging-based investigation of API concentration fluctuation caused by the sticking behaviour of pharmaceutical powder blends

Orsolya Péterfi[a], Lilla Alexandra Mészáros[a], Bence Szabó-Szőcs[a], Máté Ficzere[a], Emese Sipos[b], Attila Farkas[a], Dorián László Galata[a*], Zsombor Kristóf Nagy[a]

[a] Department of Organic Chemistry and Technology, Faculty of Chemical Technology and Biotechnology, Budapest University of Technology and Economics, Műegyetem rkp. 3., H-1111 Budapest, Hungary

[b] Department of Pharmaceutical Industry and Management, Faculty of Pharmacy, George Emil Palade University of Medicine, Pharmacy, Sciences and Technology of Targu Mures, Gheorghe Marinescu street 38, 540142 Targu Mures, Romania

* Correspondence: galata.dorian.laszlo@vbk.bme.hu; Tel.: +36 1 463 5881

Abstract

Surface powder sticking in pharmaceutical mixing vessels poses a risk to the uniformity and quality of drug formulations. This study explores methods for evaluating the amount of pharmaceutical powder mixtures adhering to the metallic surfaces. Binary powder blends consisting of amlodipine and microcrystalline cellulose (MCC) were used to investigate the effect of the mixing order on the adherence to the vessel wall. Elevated API concentrations were measured on the wall and within the dislodged material from the surface, regardless of the mixing order of the components. UV imaging was used to determine particle size and the distribution of the API on the metallic surface. The results were compared to chemical maps obtained by Raman chemical imaging. The combination of UV and VIS imaging enabled the rapid acquisition of chemical maps, covering a substantially large area representative of the analysed sample. UV imaging was also applied in tablet inspection to detect tablets that fail to meet the content uniformity criteria. The results present powder adherence as a possible source of poor content uniformity, highlighting the need for 100% inspection of pharmaceutical products to ensure product quality and safety.

Keywords

powder adhesion, machine vision, UV imaging, Raman chemical imaging, tableting, powder homogenization

1. Introduction

Content uniformity is a quality measure of the final product required by regulatory bodies, such as the European Medicines Agency (EMA) and Food and Drug Administration (FDA), to ensure product quality, efficacy, and patient safety. Patient risk is particularly important for low-dose, highly potent drugs with narrow therapeutic windows, considering that even small variations in the active pharmaceutical ingredient (API) content can lead to ineffective doses or adverse effects (Goodwin et al., 2018; Muselík et al., 2014). The main sources of failed content uniformity are

insufficient blend homogeneity, or further segregation of the initially well-mixed material during handling (Jakubowska and Ciepluch, 2021). Despite obtaining a uniform mixture, fluctuations in the API content may occur during various intermediate processes, including blending, transfer, storage, feeding, granulation, fluidization, die filling, compaction, and capsule filling (Garg et al., 2018). Furthermore, the properties of the final powder blend have a significant impact on critical quality attributes (CQA) of the final dosage form, such as dissolution profile, disintegration time, porosity, friability and hardness (Andrews, 2007).

The handling and processing of pharmaceutical materials are influenced by the sticking behaviour of the components. In the context of particle interactions, the terms sticking, agglomeration and adhesion are often used interchangeably to describe the attraction phenomenon between two solid bodies with a common contact surface (Petean and Aguiar, 2015; Zimon, 1982). The adhesion forces between particles and surfaces come as a result of electrostatic forces, capillary forces and van der Waals forces, among others (Beaudoin et al., 2015; Salazar-Banda et al., 2007). On the other hand, cohesion refers to the chemical forces holding similar particles together (Frabetti et al., 2021).

The quality of the final pharmaceutical product is influenced by the various factors that impact the adhesion and cohesion interactions of pharmaceutical powders. The surface roughness and the topography of the equipment directly affects the contact area between particles and the surface (Karner et al., 2014; Mazel et al., 2013; Wang et al., 2015). The sticking behaviour also depends on the material properties, such as the surface area, the polymorphic form and crystal morphology of the powder (Abdel-Hamid et al., 2011; Capece, 2019; Paul et al., 2020; Waknis et al., 2014). The adhesion of small particles on rough surfaces is primarily determined by the geometrical effects between the surface-particle system. In contrast, particles larger than the surface features have multiple contact areas, with both particle size and surface roughness significantly influencing adhesion (Katainen et al., 2006). Humidity causes the formation of liquid bridges and increases in the removal force, thereby altering the flow and adhesion behaviour of the material (Stevenson et al., 2023).

Previous studies have investigated the undesirable effect of powder adhesion during tableting and capsule filling. Punch sticking occurs when an API or excipient exhibits a stronger affinity for tablet punches (adhesion) than for the components of the formulation (cohesion), leading to tablet defects, manufacturing downtime, and yield losses (Chattoraj et al., 2018; Simmons, 2019; Simmons and Gierer, 2012; Takeuchi et al., 2020). Stickiness during the encapsulation process causes a large variability in capsule fill weight, and the repeated contact between the powder and metal parts may significantly affect machine performance (Podczeck, 2004). Even when utilizing excipients with satisfactory flow properties, such as microcrystalline cellulose (MCC), the phenomenon of powder sticking to the walls of the dosing nozzle has been observed (Patel and Podczeck, 1996; Tan and Newton, 1990). In the effort to mitigate adhesion to the tooling, lubricants are most often applied, however these may hinder drug dissolution (Abe and Otsuka, 2012; Uzunović and Vranić, 2007). Podzeck explored an alternative solution by modifying the stainless-steel surface of the tamping pins with various metal coatings (Podczeck, 1999).

Several experimental methods have been developed to detect and measure surface-powder interactions. The methods can be categorized into qualitative and quantitative techniques, each offering valuable insights into powder adhesion, thereby providing a more comprehensive

understanding of the sticking phenomenon. Quantitative methods involve the direct measurement of the magnitude of powder adherence. In the centrifugal technique, particles deposited on the substrate detach during centrifugation. Image analysis is used to determine the number of adhered particles before and after centrifugation; the results are then analysed statistically to determine the average adhesion force (Booth and Newton, 1987; Petean and Aguiar, 2015; Thomas and Beaudoin, 2015). The development of the colloid-probe atomic force microscopy (AFM) allowed the investigation of surface forces between a single particle and the surface (Bunker et al., 2011; Ibrahim et al., 2000; Preedy et al., 2015). Imaging techniques have been previously used as qualitative measure of powder adhesion to compression tools. Scanning electron microscopy (SEM) and energy dispersive X-ray spectroscopy (EDS) can visualize the material adhering to the tablet punches (McDermott et al., 2011; Neilly et al., 2009; Tsosie et al., 2017). Rhodes et al. utilized Raman chemical imaging to examine the material residue on the punch surface (Rhodes et al., 2022). Mollereau et al. used image analysis to detect and quantify the visual defects caused by tablet sticking (Mollereau et al., 2013). The aforementioned imaging techniques were primarily utilized for detecting tablet sticking; their suitability in the analysis of powder adherence during other pharmaceutical processes remains unexplored.

Recent advancements in machine vision technology provide a fast and cost-efficient approach for quality control and process monitoring in the pharmaceutical industry (Galata et al., 2021). In a study conducted by Wu et al., multispectral UV imaging was employed to visualize drug and excipient distribution in tablets containing glibenclamide, MCC and magnesium stearate (Wu et al., 2014). The versatility of this imaging technique has been demonstrated in various pharmaceutical applications, such as the surface analysis of multiple unit pellet systems (MUPS) (Novikova et al., 2016), determining tablet coating thickness (Novikova et al., 2017) and estimating tablet hardness and API content (Klukkert et al., 2016). Multispectral UV imaging was applied to detect tablets with inhomogeneous surface density (Klukkert et al., 2016). Mészáros et al. increased image acquisition speed by utilizing UV imaging exclusively in the 380–395 nm range. The technique was successfully used to determine API content and particle size from meloxicam tablets, a yellow model drug (Mészáros et al., 2022, 2020). However, these novel imaging methods have not yet been utilized to characterize powder adherence to the wall of manufacturing equipment. These imaging techniques can greatly contribute to the understanding of the sticking behaviour of pharmaceutical powders, the information gained this way can be used to prevent future inhomogeneity problems.

This article aims to explore methods for examining the sticking behaviour of pharmaceutical powder blends to stainless-steel surfaces during the homogenization process. The combination of quantitative methods and imaging techniques provides a more complex understanding of powder adherence. A comprehensive review of the relevant literature revealed that no results have been published up to now regarding the use of chemical imaging techniques to investigate powder adhesion to the surface of pharmaceutical equipment. Accordingly, the present work focused on the use of UV imaging to determine the distribution and particle size of the API particles. The feasibility of UV imaging to predict the tablet API content was also explored, contributing to the integration of machine vision into pharmaceutical quality control. The specific objectives include quantifying the API content in the powder adhering to the mixing vessel walls, assessing the importance of different mixing orders, and determining the API content in the material detached from the metallic surface. Rapid chemical imaging techniques such as UV-VIS imaging were employed to evaluate the distribution and particle size of the API on stainless-steel surfaces. To

the authors knowledge, this is the first time that UV imaging has been used to characterize the adhesion of pharmaceutical particles to stainless-steel surfaces. Furthermore, we also intend to utilize UV imaging to detect tablets that deviate from the target API content.

The binary powder mixture selected for this investigation contained amlodipine as model API and MCC as multipurpose excipient. Amlodipine is an antihypertensive and antiischemic drug with poor manufacturability, attributed to the sticking behaviour and unfavourable flow properties of the material. In contrast, MCC is a versatile pharmaceutical excipient used in tablets, capsules, pellets and granule formulations due to its excellent flow properties and good compressibility. Our aim was to explore methods for examining the sticking behaviour of pharmaceutical powder blends to stainless-steel surfaces during the homogenization process. The dislodgment of the material from the metallic surface due to a mechanical impact may lead to small volumes where API concentration deviates from the average value, potentially resulting in products with poor content uniformity. Detecting these outliers proves challenging with traditional analytical methods, emphasizing the importance of 100% quality control during the manufacturing process.

2. Materials and methods

2.1. Materials

Amlodipine besylate was purchased from Sigma-Aldrich. The API particles were ground in a mortar to obtain fine amlodipine. Microcrystalline cellulose (Vivapur 200) was obtained from JRS Pharma (Rosenberg, Germany). The physical properties for each powder are provided in Table 1.

Table 1: The physical properties of the materials

Material	Bulk density (g/cm^3)	Angle of repose (°)	Carr classification of flowability
MCC	0.37	35.5	Free flowing
Original amlodipine	0.30	68.9	Very cohesive, non-flowing
Fine amlodipine	0.35	39.0	Fair to passable flow

2.2. Methods for investigating adhesion to the wall surfaces

Binary powder mixtures were prepared with 2.5% (w/w) amlodipine concentration. The study of material adherence was carried out through the application of two primary methods. Adhesion is known to be highly sensitive to humidity and temperature, therefore the experimental environment was kept consistent for all experiments at 25°C and 40% RH.

2.2.1. Adherence during powder homogenization

Powder adherence was examined in a QUICKmill Lab multifunctional mixing apparatus (Quick2000 Ltd., Tiszavasvári, Hungary) equipped with a 1.5 L stainless-steel mixing vessel. The vessel was rotated at 15 rpm in all experiments. The following four methods were applied during homogenization:

1. Initially MCC is rotated in the mixing tank for 5 min, followed by the addition of amlodipine, and the subsequent homogenization of the mixture for 10 min. Henceforth, this sample is called M1.
2. Initially, amlodipine is rotated in the mixing tank for 5 min, then MCC is added and the mixture is homogenized for 10 minutes. Hereafter, the sample is named A1.
3. Amlodipine and MCC are poured into the mixing vessel, and then mixed together for 10 min. This sample is called T1.
4. Fine amlodipine powder and MCC are placed into the mixing vessel, and then mixed together for 10 min. This sample is named T2.

After the homogenization, the mixture was discharged and samples were collected from the bottom, middle, and top layers within the container. The sample was discharged through the bottom orifice of the vessel onto a moving conveyor belt, therefore the powder formed a line on the conveyor belt. The front of the line corresponded with the bottom of the sample, while the top of the sample was located at the end. Three samples were obtained from each respective location. Subsequently, the material adhered to the inner wall of the container was dislodged by hitting each side of the mixing tank once with a rubber mallet, then the samples were collected. The amlodipine concentration of the samples was determined via UV spectroscopy.

100 mg of each sample obtained during powder homogenization described in section 2.2.1. (top, middle, bottom layer and dislodged material) were directly compressed into tablets at 5 kN compression force using a Dott Bonapace Cpr6 (Dott Bonapace, Limbiate, Italy) eccentric tablet press, equipped with an 8 mm flat punch. The tablets were analysed using Raman mapping and UV imaging.

2.2.2. Adherence to a stainless-steel plate

Powder adherence to a stainless-steel plate was investigated by submerging the plate into different samples, with the lid of the mixing tank serving as the stainless-steel plate. The plate was consistently immersed up to a previously marked line, ensuring the same surface area during each experiment (22.2 cm^2).

Initially, the plate was immersed in MCC and subsequently in the amlodipine-MCC mixture (sample PM1). In the second instance, the plate was first dipped in amlodipine and then in the homogenized mixture (sample PA1). In the third case, the plate was directly immersed in the original amlodipine-MCC mixture (sample PT1), while in the fourth instance, it was placed in a mixture with MCC and fine amlodipine powder (sample PT2).

The material adhering to the plate was examined using Raman chemical mapping. UV imaging was employed to capture images after immersing the plates in the samples and after dislodging the powder using a rubber mallet. The total mass of the adhered material on the plates was measured.

The surface was rinsed with distilled water and any adherent particles were washed into a volumetric flask. The concentration of the API was determined using UV spectroscopy, each measurement was performed with three replicate samples. After each experiment, the stainless-steel surface was cleaned using acetone.

2.3. Measurement of the API content by UV spectroscopy

An Agilent 8453 UV/VIS spectrometer (Hewlett-Packard, CA, USA) was used to measure the API content at 242 nm in a 10 mm cuvette. The sample was accurately weighed and dissolved in a volumetric flask with distilled water. In the case of the mixing tank, about 0.1 g sample was placed in a 250 mL volumetric flask. The adherence of the powder to the stainless-steel plate was examined by measuring the plate's mass before and after immersing into the samples. The surface was rinsed with distilled water to collect all of the powder from the plate surface and the resulting solution was diluted in a 25 mL flask. The flasks were placed on magnetic stirrers at 200 rpm for 30 min. Prior to measurement, an adequate volume was filtered through a 1.2 µm filter (FilterBio® GF Syringe Filter, Labex Ltd., Budapest, Hungary) and the first 5 mL was discarded.

2.4. Raman mapping

Raman imaging of the stainless-steel plate surface and the tablets was performed using a Horiba Jobin-Yvon LabRAM system (Longjumeau, France). Spectra were recorded with a 785 nm, 80 mW diode laser focused on the sample through an Olympus BX-40 optical microscope with an objective of 20 times magnification. The spectral region of 200–3600 cm^{-1} was covered. Each spectrum was collected with an acquisition time of 5 s and 2 spectra were averaged at each location. In the centre of the metal plate, an 1.6 mm × 1.6 mm region was mapped, using an 81 × 81 grid size with a step distance of 20 µm. The total mapping cycle for a sample took approximately 19 h.

Data analysis was performed in MATLAB 2022a (Mathworks, Natick, MA, USA) equipped with the PLS_Toolbox 7.8.2. (Eigenvector Research, USA). The Raman spectra were pre-processed with automatic Whittaker baseline correction (asymmetry=0.001, lambda=10000) and normalization. Classical least squares (CLS) with the non-negative least squares (NNLS) algorithm was used to create the chemical map of the samples. The Raman spectra of amlodipine, MCC and the stainless-steel plate were used as reference spectra.

2.5. Image acquisition with UV imaging

Images of the samples were captured using a Canon 650D DSLR camera (Canon, Japan) and Canon EFS 18–55 macro lens (Canon, Japan) secured with a reversing ring. The camera was coupled with a computer via a USB 3.0 interface. The ring light connected to the objective lens contained one row of UV light-emitting diodes emitting in the 380–395 nm range (Apokromat Ltd, Hungary). Images were captured from both sides of the tablets with a resolution of 3456 × 5184 pixels at an ISO-400 setting. A QPCard 101 v3 millimeter reference scale (Argraph Corp., NJ, USA) was used to calibrate the system. After calibration, each pixel represented a size of 1.1765 µm for stainless-steel plate measurements and the shutter speed was set to 10 ms. In the case of tablets, the pixel size was 2.778 µm, with an exposure time of 1.5625 ms. VIS images were captured with a shutter speed of 0.6 seconds using a ring light with three rows of white light emitting diodes (Apokromat Ltd., Hungary).

2.6. Image analysis

Image analysis algorithms were developed in MATLAB 2022a (Mathworks, Natick, MA, USA). Two distinct algorithms were employed to retrieve the required data from the UV images: one focused on particle size analysis, while the other was utilized to determine the API content within the tablets.

2.6.1. Colour analysis of the tablets

Circular Hough transform was used to separate the coloured pixels of the tablets from the background. During colour analysis the RGB colour space was used, which relies on the additive combination of its three primary colours—Red, Green, and Blue –to represent various colours (for example black is represented by R = G = B = 0 and white by R = G = B = 255).

The B values (blue in RGB colour space) were used for colour analysis because the API and excipient were easily distinguished in the B channel due to the distinctive blue colour of the API under UV illumination. The average B value of the 2 images belonging to a tablet was calculated from the B value histograms (one image from each side of the tablet). These values were used to create a simple univariate calibration to predict API content.

2.6.2. Particle size analysis

Figure 1. summarizes the main steps of image processing. The first step was converting the true colour image (RGB) into grayscale, then a Gaussian filter was used to reduce the noise and/or blurring caused during the capturing of the images. Images were binarized by assigning pixels below a defined threshold to 0, while those above were set to 1, thereby distinguishing between the background and foreground. The aforementioned steps involve adjustable parameters (sigma, threshold value) which were iteratively tested to find the optimal values.

Edge detection was utilized to identify particle boundaries, allowing for the subsequent determination of the equivalent circular diameter and convexity of the objects. Particle overlap was inevitable during UV imaging, which could skew the particle size distributions towards large particles. Images revealed that the API was in the form of prismatic crystals without any agglomeration. Consequently, particles demonstrating low convexity (<0.95) were presumed to be overlapping particles rather than agglomerates and were therefore removed from the dataset. Particles touching the image borders were also excluded from the analysis.

The equivalent circular diameter of the particles was initially determined in pixels, and subsequently converted to micrometres. The experimental data was expressed in volume-based particle size distribution (PSD) and average diameters (D_{10}, D_{50}, D_{90}) were also calculated.

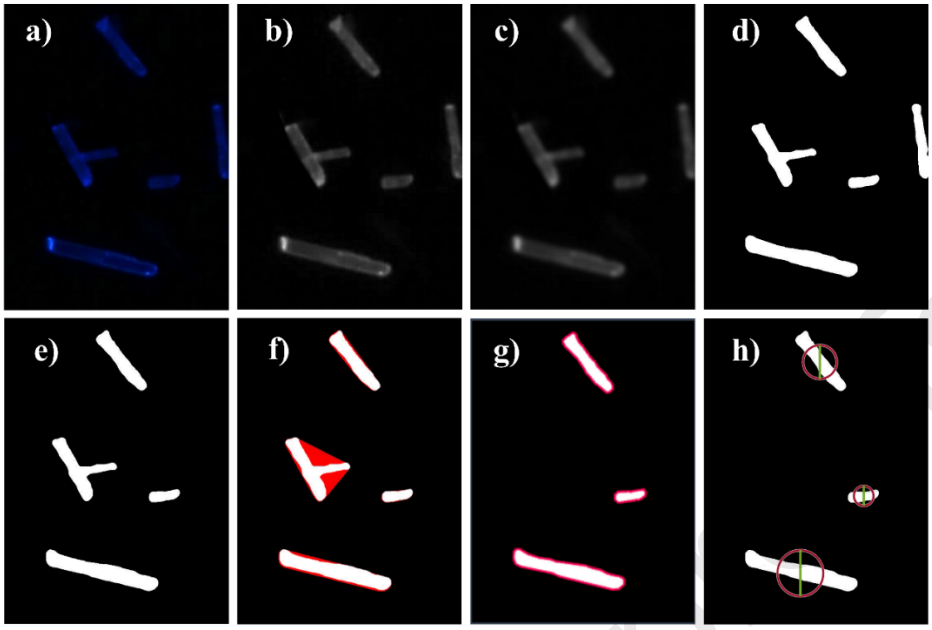

Figure 1: Main steps of image processing: (a) original image, (b) converting to grayscale, (c) Gaussian blur, (d) thresholding (binarization), (e) removing objects touching the borders, (f) removing objects with low convexity (<0.95), (g) contouring objects (edge detection) and calculating equivalent diameter.

Images of the tablets were resized to 70% of their original size, which allowed for the reduction of image processing time. Background extraction implemented Hough circle transform to remove of any undesirable objects from the background. The same image analysis process steps were used to determine the API particle size in the tablets (Figure 2.).

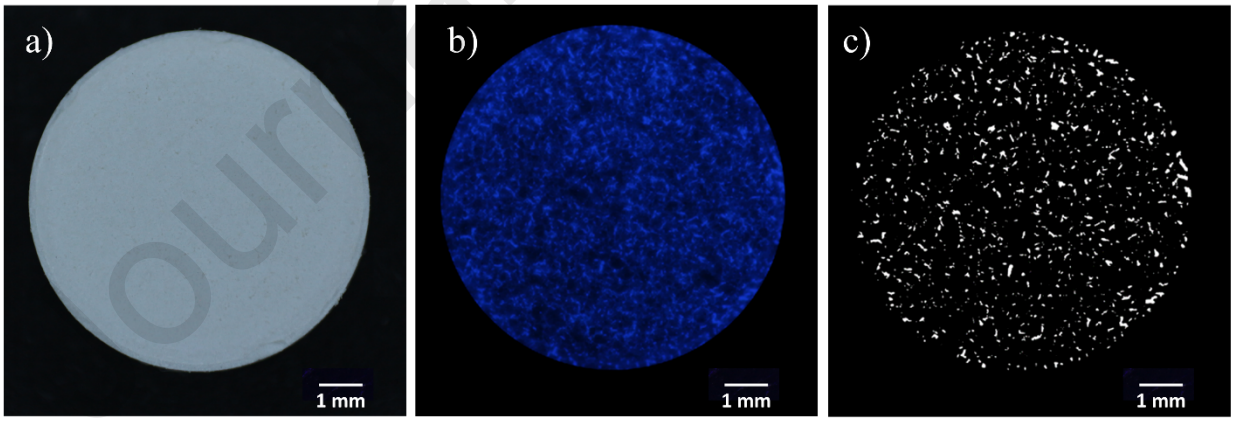

Figure 2: The acquired images from the same tablet: (a) using VIS illumination, (b) using UV illumination, (c) UV image after image processing.

3. Results and discussion

A comprehensive review of the relevant literature revealed that no results have been published up to now regarding the use of chemical imaging techniques to investigate powder adhesion to the surface of pharmaceutical equipment. Accordingly, the present work focused on the use of UV imaging to determine the distribution and particle size of the API particles. The feasibility of UV imaging to predict the tablet API content was also explored, contributing to the integration of machine vision into pharmaceutical quality control.

The binary powder mixture selected for this investigation contained amlodipine as model API and MCC as multipurpose excipient. Amlodipine is an antihypertensive and antiischemic drug with poor manufacturability, attributed to the sticking behaviour and unfavourable flow properties of the material. In contract, MCC is a versatile pharmaceutical excipient used in tablets, capsules, pellets and granule formulations due to its excellent flow properties and good compressibility. Our aim was to assess the potential API content variations between the homogenized mixture and the material adhering to the wall of the mixing vessel. The dislodgment of the material from the metallic surface due to a mechanical impact may lead to small volumes where API concentration deviates from the average value, potentially resulting in products with poor content uniformity. Detecting these outliers proves challenging with traditional analytical methods, emphasizing the importance of 100% quality control during the manufacturing process.

3.1. Adherence to the wall of the mixing vessel during powder homogenization

To investigate the adherence phenomenon during powder homogenization, three experiments were conducted, altering the order of component mixing during the preparation of the amlodipine-MCC mixture. Additionally, another blend was formulated with fine amlodipine powder. Three samples were collected from every sampling location. Table 2. summarizes the measured API concentrations for each sample obtained from the mixing tank.

Table 2: Average amlodipine concentration (± standard deviation of the three measurements) in the samples obtained from powders homogenized with various methods

Sample	Sampling location			
	Bottom	Middle	Top	Dislodged material
M1	2.52 ± 0.05 %	2.52 ± 0.01 %	2.53 ± 0.03 %	4.41 ± 0.10 %
A1	2.16 ± 0.06 %	2.11 ± 0.10 %	2.11 ± 0.06 %	9.77 ± 0.31 %
T1	2.54 ± 0.04 %	2.60 ± 0.05 %	2.49 ± 0.01 %	3.72 ± 0.19 %
T2	2.51 ± 0.04 %	2.49 ± 0.03 %	2.46 ± 0.02 %	4.95 ± 0.12 %

The results indicate the concentration of amlodipine within the main mass of the homogenized powder mixture was close to the theoretical concentration of 2.5% except for sample A1. When amlodipine was initially rotated alone in the mixing vessel, the amlodipine concentration in the main mass of the homogenized powder is significantly lower, around 2.12%. This suggests the adherence of a substantial amount of API to the wall, when amlodipine was initially rotated alone in the mixing tank. Only minor differences were observed between the bottom, middle, and top of the homogenized mixtures.

Subsequently, the material adhered to the inner wall of the container was dislodged by hitting each side of the mixing tank once with a rubber mallet, then the samples were collected. The material dislodged from the wall contained significantly higher quantities of amlodipine compared to the nominal concentration. The results indicate that the concentration strongly depends on the mixing order. Introducing both components simultaneously into the vessel resulted in an API concentration of 3.72%, marking the lowest concentration among the four studied cases, despite the increase compared to the homogenized mixture. However, when utilizing fine amlodipine particles, a higher concentration of the active ingredient (4.95 ± 0.12 %) was measured in the dislodged sample.

The highest concentration of amlodipine in the dislodged material was measured when amlodipine was initially rotated in the mixing vessel, allowing for a larger free surface area for the API. This resulted in less adherence of MCC when introduced later in the process. Interestingly, even when MCC is the initial component rotated in the vessel, it did not hinder the accumulation of amlodipine on the wall. In this instance, the concentration of amlodipine on the wall surpasses that observed when both components were added simultaneously.

Knowing the mass of the material dislodged from the wall of the mixing tank allows the calculation of how much material was dislodged per unit surface area. It is evident that not only does the concentration of adhered material change, but the total quantity of material also differs among the various cases. When the MCC was initially added to the mixing tank, the quantity of the dislodged material was lower (2.18 g/m^2) than when both components were added (2.48 g/m^2). The smallest amount of material was dislodged when fine amlodipine was used during the homogenization (1.89 g/m^2). Notably, the most amount of material was collected when amlodipine was first rotated in the tank (8.82 g/m^2).

Despite a relatively small quantity of material falling off the surface of the homogenizing equipment, it can lead to small volumes where API concentration deviates from the target value, particularly when it occurs towards the end of homogenization process. As a result, certain tablets or capsules manufactured under these conditions may not meet the required standards. With only a few outliers in each batch, the detection of these outliers is unlikely with the currently applied analytical methods. This still poses a potential risk for the patient especially in the case of APIs with low therapeutic indices. Thus, a comprehensive quality inspection of the entire batch is imperative.

3.2. Adherence to stainless-steel plate

Investigating the adherence of the API to the wall of the mixing vessel during homogenization may require more material, especially when testing multiple cases. Alternatively, assessing the adherence of the materials to a stainless-steel plate by immersing in the sample provides an alternative approach to examine the adherence of the constituents. Table 3. summarizes the amlodipine concentration of the powder adhered to the stainless-steel plate. The results follow a similar trend as observed in the case of material dislodged from the wall of the mixing vessel. The lowest concentration of amlodipine was obtained when the steel plate was immersed solely in the pre-homogenized mixture. In the case of the pre-homogenized mixture containing fine API, the concentration of amlodipine on the plate was higher compared to the original mixture. Moreover, the API concentration nearly doubles when the plate is immersed in amlodipine first. The amlodipine concentration in the dislodged material, obtained after homogenization in the mixing tank, was found to be lower than the amlodipine concentration in the material adhered to the stainless-steel plate. The API concentration in the dislodged material from the stainless-steel plate was higher compared to that observed in the dislodged material from the mixing vessel wall. The concentration difference may be attributed to the more intensive detachment of particles from the walls during homogenization in the mixing vessel. However, despite these concentration differences, a consistent trend was observed among various samples, indicating that the adherence behaviour in various experimental conditions could be assessed by immersing the steel plate in the analysed sample.

Table 3: Amlodipine concentration in the various samples during the stainless-steel plate experiments

Sample	**Amlodipine concentration (w/w%) in:**

	the total material adhering to the steel plate	the material remaining on the steel plate after a mechanical impact	the dislodged material
PM1	24.07 ± 2.12 %	32.35 ± 1.65 %	4.46 ± 0.22 %
PA1	55.34 ± 2.15 %	81.50 ± 5.05 %	10.49 ± 0.54 %
PT1	19.45 ± 1.55 %	27.06 ± 2.03 %	3.95 ± 0.12 %
PT2	28.02 ± 2.01 %	37.95 ± 2.20 %	5.21 ± 0.25 %

UV spectroscopy allowed for the quantitative comparison of the various homogenization cases. Complementary to this, imaging techniques were employed to investigate the adherence of the powder mixture to the stainless-steel plate, offering detailed insights into the distribution and particle size of the API on the surface.

Distinguishing between the two components under VIS light is not feasible due to their similar white to off-white colour. Amlodipine exhibits native fluorescence and appears bright blue under UV illumination. MCC particles lack this characteristic, and as a result, the contrast in colour between the amlodipine particles and the MCC is stronger under UV light. Figure 3. shows the images acquired from the same area on the steel plate immediately after immersing the plate in the pre-homogenized mixture and after dislodging the material with a rubber mallet. Images were obtained under visible light and UV illumination in order to visualise the effects of dislodging the material due to a mechanical impact. The visual examination of the images reveals the dislodgement of the larger MCC and amlodipine particles from the metallic surface. Nevertheless, a portion of the larger API crystals still remained on the surface.

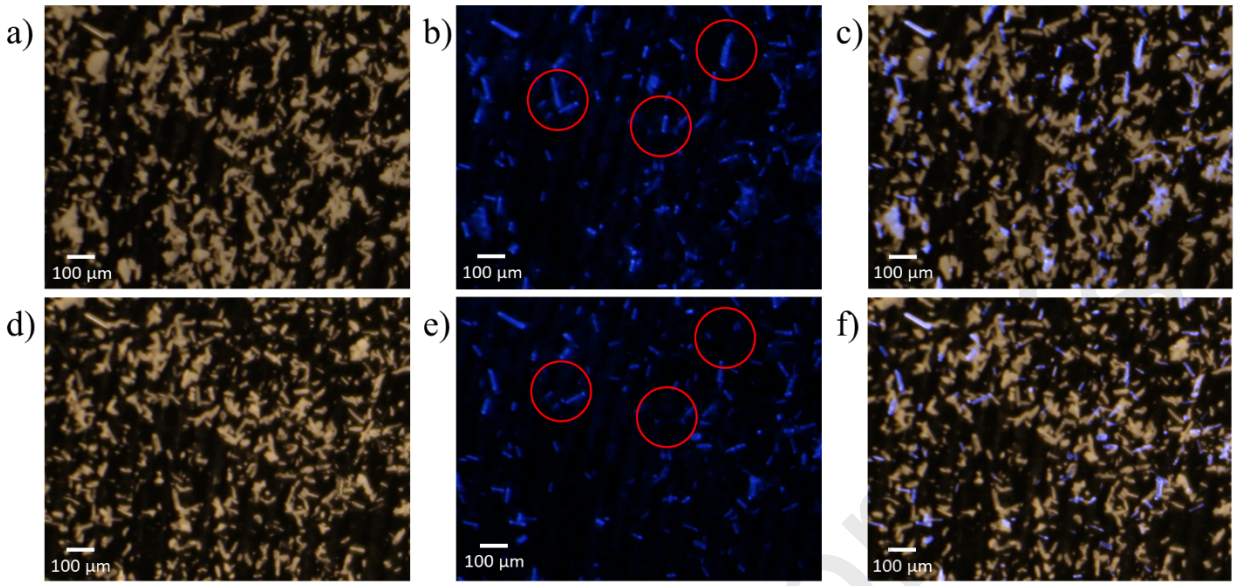

Figure 3: Visualisation of the same area on the steel plate under various conditions: (a) immediately after immersing in the pre-homogenized mixture with VIS illumination, (b) under UV illumination (b) and (c) a combined visualization of both. Additionally, (d) showcases the area after material dislodgment with VIS illumination, (e) under UV illumination, and (f) incorporates both images obtained with VIS and UV illuminations.

Figure 4. shows the images obtained with UV imaging after immersing the stainless-steel plate in the powder mixtures. The images allow for the investigation of the distribution of the API on the surface. Samples PM1, PA1, and PT1, prepared with the original amlodipine mixture, contained predominantly needle-like particles. Smaller equant-shaped crystals were present when the steel plate was immersed in the fine amlodipine-containing mixture (sample PT2). There was a noticeable reduction in the adhesion of the API to the surface when the stainless-steel plate was immersed in MCC prior to the pre-homogenized mixture. In contrast, when the steel plate was immersed in the API first, amlodipine covered a substantial portion of the surface (Figure 4. b). It is also noteworthy that in the case of fine amlodipine, the distribution of the API on the surface is more uniform. The smaller mass of the adhered material in this case can be explained by a layer of fine particles uniformly coating the steel plate, preventing further particle adhesion.

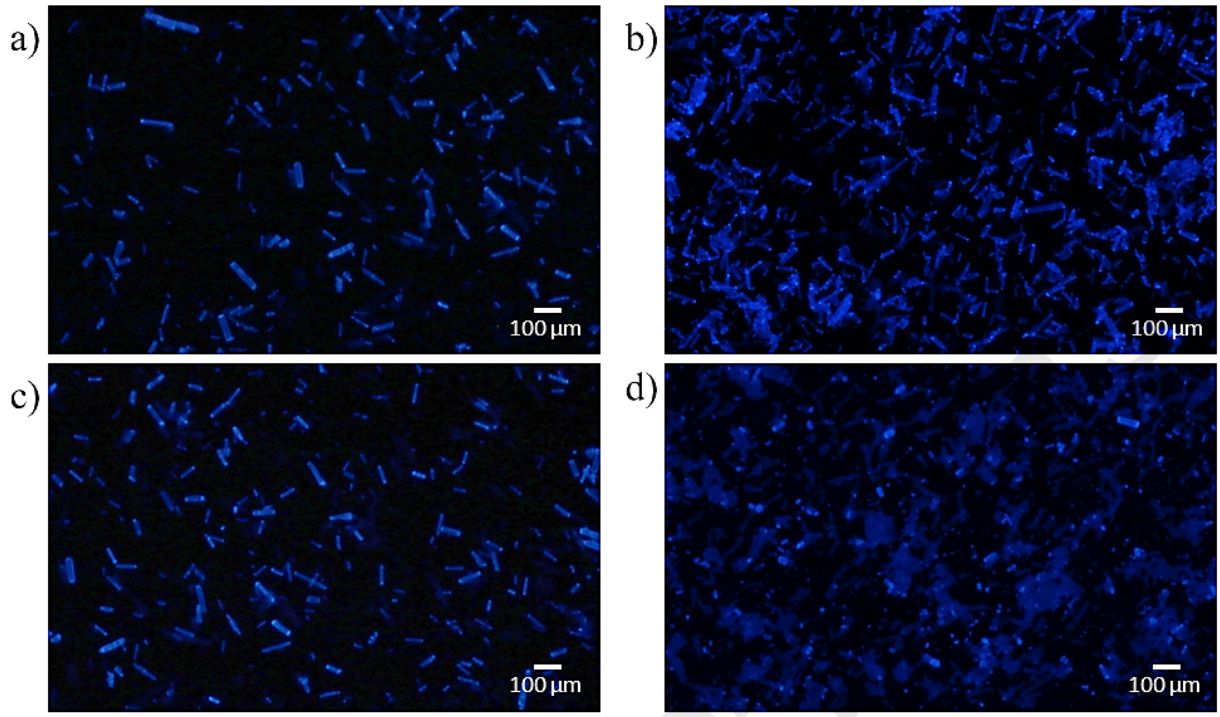

Figure 4: Images obtained with UV imaging after immersing the stainless-steel plate in the powder mixture in various orders: a) PM1, b) PA1, c) PT1, d) PT2.

For comparison, Raman mapping of the samples was also performed. The obtained maps are shown in Figure 5. The distribution of the API on the metal surface was similar to UV imaging, with comparable particle size and shape characteristics observed between the two methods. The Raman mapping of the 1.6 mm × 1.6 mm region took approximately 19 h per sample. In contrast, the machine vision-based system enabled the acquisition of high-resolution images of the samples (3456 × 5184 pixels) in only a few milliseconds.

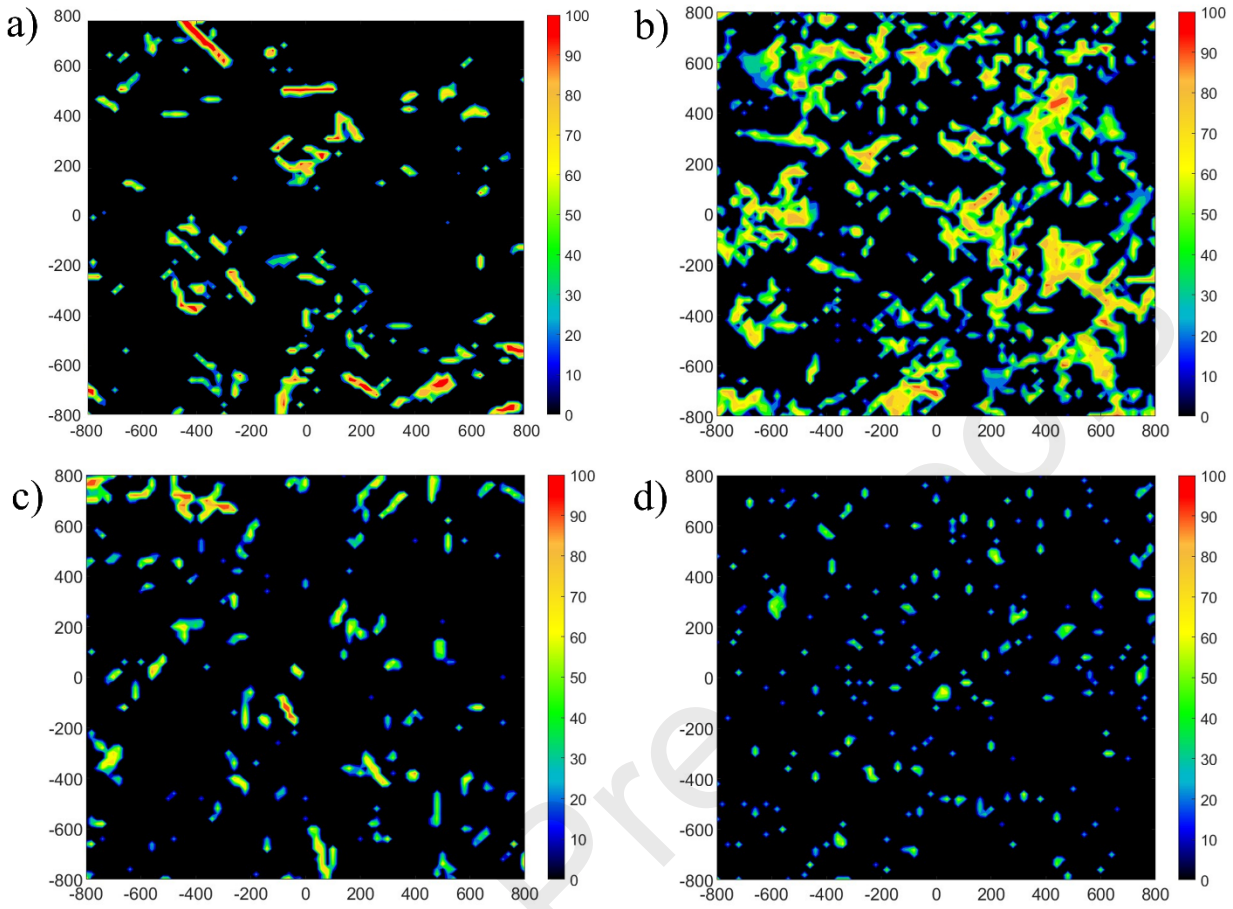

Figure 5: Raman maps of the PM1 (a), PA1 (b), PT1 (c) and PT2 (d) samples. The left and bottom axes depict the distance relative to the centre in micrometres. The colourbars represent the amlodipine concentration predicted by the CLS method.

Both UV imaging and Raman mapping are valuable tools for acquiring chemical maps. In Figure 6., a comparison between the microscopic image and the Raman chemical map of the PT2 sample is presented. Additionally, Figure 7. provides a comparative analysis of the VIS image and the chemical map obtained by combining the VIS and UV images. UV imaging enables the rapid acquisition of chemical maps, covering a substantially large area representative of the analysed sample.

A similar distribution of the powder constituents was observed on both chemical maps, however the API particles appeared smaller in the case of UV imaging. This may be attributed to the decreased resolution of the Raman maps where a pixel occupies a larger area on the image, leading to the apparent size difference. UV imaging also allowed for the detection of small API particles adhering to the MCC particles. In the case of the Raman maps, such fine particles were seldom detected, possibly due to the step distance of 20 µm. The MCC signal could also contribute to masking the signal of these fine amlodipine particles in the Raman maps. While UV imaging has been utilized with only two components, where only one component is visible under UV illumination, its potential expands to multicomponent systems. In such cases, where several components exhibit UV activity, UV imaging could be effectively employed using light sources

with various wavelengths, enabling the separate detection of different substances. Nonetheless, differentiation of certain substances may not be possible under UV illumination.

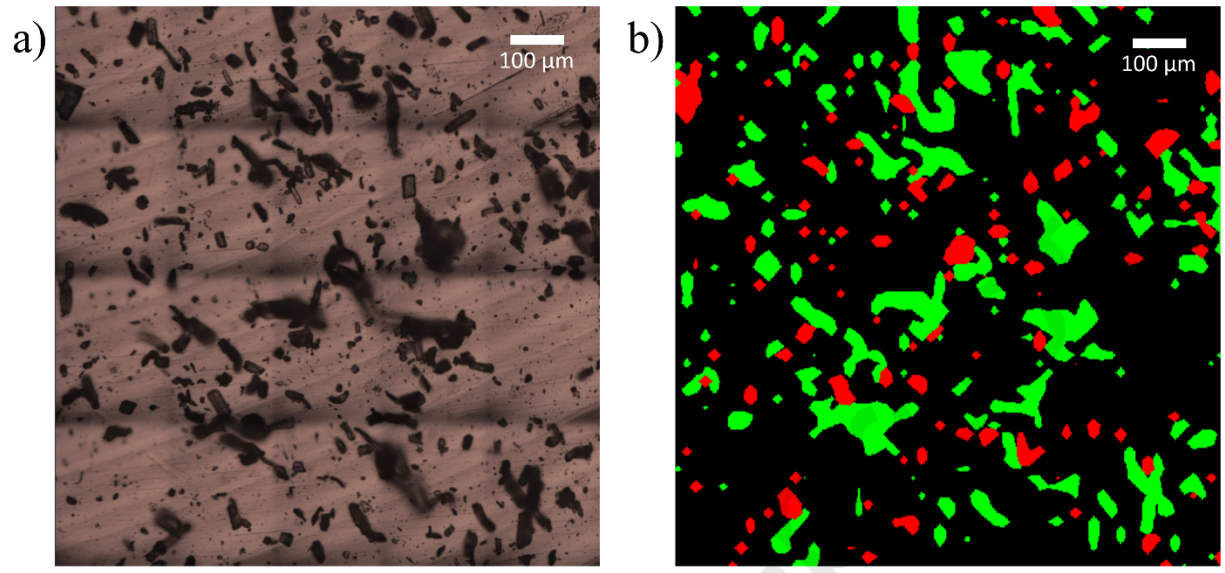

Figure 6: Comparison of the microscopic image (a) and the Raman chemical map (b) of the same area of the PT2 sample. The MCC particles are coloured green, while amlodipine is represented with red.

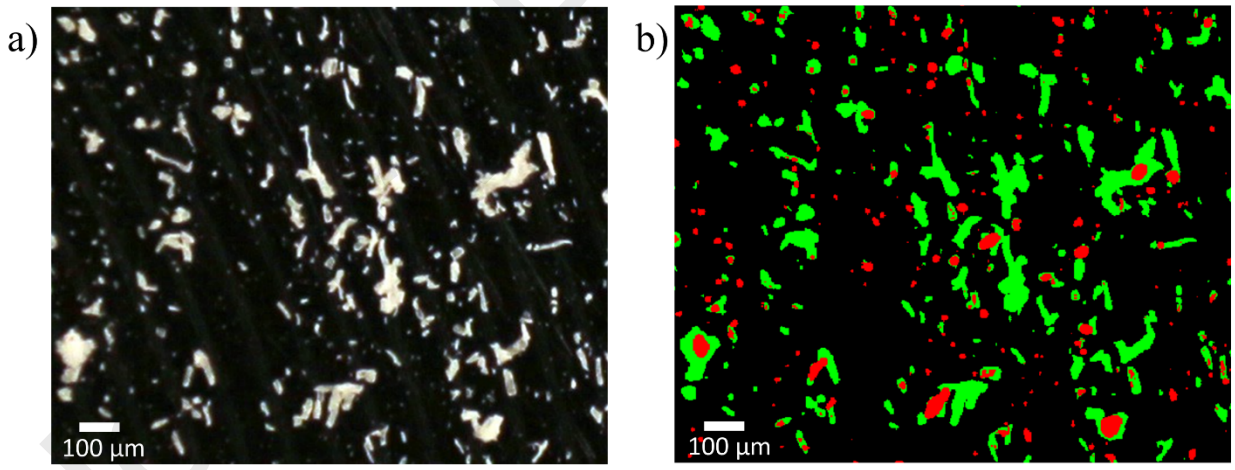

Figure 7: Comparison of the VIS image (a) and the chemical map obtained with UV imaging (b) of the same area of the PT2 sample. The MCC particles are coloured green, while amlodipine is represented with red.

3.3. Particle size analysis

The dissolution of a pharmaceutical product is significantly influenced by particle size distribution (PSD) of the API (Chu et al., 2012). Although API particle size may change between batches, segregation of the material can also cause localized areas with different sized material. Conducting

particle size analysis of the samples during various manufacturing steps ensures product quality and safety (Stauffer et al., 2018; Zakhvatayeva et al., 2019).

A comparative analysis of the particle size of various samples aimed to determine the potential difference between the particle size of the material adhering to the wall of the mixing tank, the material remaining on the surface after a mechanical impact and the material in the homogenized mixture. The PSDs and corresponding statistical values were obtained from all the images of the T1, T2, PT1 and PT2 samples, and are presented in Figure 8. and Table 4.

The PSD of amlodipine was determined by evenly distributing the sample and analyzing the acquired images. The analysis of the steel plate gave information about the particle size of the API adhering to the surface (PT1.1 and PT2.1) and remaining on the plate after a mechanical impact (PT1.2 and PT2.2). Furthermore, the amlodipine particle size was determined from the tablets obtained from the homogenized mixtures (T1.1 and T2.1) and from the material dislodged from the wall of the mixing tank after a mechanical impact (T1.2 and T2.2). Considering the statistical values in Table 4., there was no discernible difference between the D_{10}, D_{50} and D_{90} values of the various samples. Notably, similar trends were observed across the PSDs acquired from tablets and from the material adhering to the surface of the steel plate. The machine vision-based method was suitable for differentiating between the samples prepared with different-sized API and it yielded valuable information regarding the particle size of material adhering to the surface.

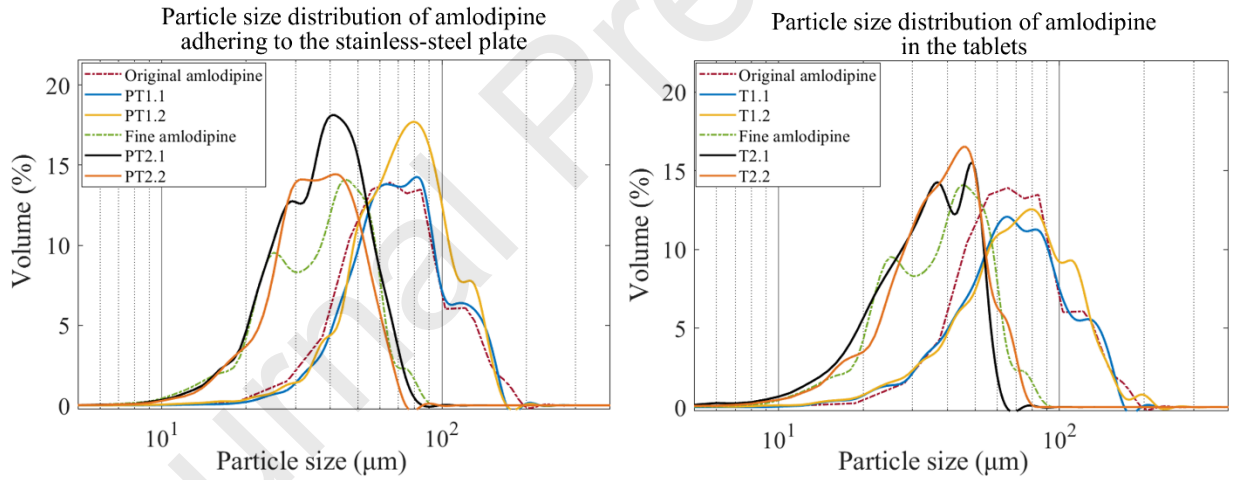

Figure 8: Particle size distribution (PSD) of amlodipine in the various samples measured on the stainless-steel plate and from the tablets.

Table 4: The calculated statistical values of PSDs based on the acquired UV images of the T1, T2, PT1 and PT2 samples

Sample	Description	D_{10}	D_{50}	D_{90}	Span
Original amlodipine	It was used in the preparation of sample T1 and PT1.	40.15	66.54	117.35	1.16
PT1.1	API adhering to the steel plate (PT1 sample)	42.47	70.01	120.17	1.11
PT1.2	API adhering to the steel plate after mechanical impact (PT1 sample)	43.27	73.33	118.40	1.03
T1.1	Tablet from the homogenized mixture (T1 sample)	35.87	67.83	119.78	1.24
T1.2	Tablet from the dislodged material (T1 sample)	35.52	71.36	119.54	1.18
Fine amlodipine	It was used in the preparation of sample T2 and PT2.	20.57	38.24	57.44	0.96
PT2.1	API adhering to the steel plate (PT2 sample)	21.61	37.58	56.60	0.93
PT2.2	API adhering to the steel plate after mechanical impact (PT2 sample)	21.26	35.57	53.55	0.91
T2.1	Tablet from the homogenized mixture (T2 sample)	17.82	34.92	50.10	0.95
T2.2	Tablet from the dislodged material (T2 sample)	20.31	37.63	56.12	0.95

3.4. Colour analysis of the tablets

The feasibility of UV imaging was evaluated for predicting the drug content of the tablets containing amlodipine. The average B value for each tablet was determined by analysing the pixel values of the acquired images under UV illumination, incorporating data from both sides of the tablet. Figure 9. demonstrates the relationship between the average B values of the samples and the nominal amlodipine concentration of the tablets.

Amlodipine particles exhibit higher B values than the MCC particles, therefore an increase in the API content of the tablets corresponds to an elevated average B value. The tablets from the homogenized mixture of the A1 sample contained less amlodipine, resulting in lower B values. However, at higher concentrations the relationship becomes non-linear, a phenomenon attributed to the saturation of B values. The application of B values to classify tablets offers a means to identify outliers that may arise during tablet manufacturing.

A simple univariate model was created with the use of the average B values of the tablets. Three samples were used to test the model and, therefore were not included in the model: one M1 tablet from the homogenized mixture, one A1 tablet from the homogenized mixture and the tablet from the dislodged material of sample T1. The resulting equation, based on a power function of the second-order, yielded an R^2 value of 0.9531:

$$Concentration = \ -2.379 * 10^{-9} * (average\ B\ value)^{4.308} + 1.649$$

The built calibration model was used to determine the nominal API content of the samples. The root mean squared error of prediction (RMSEP) for the three test samples was 0.144 w/w% API. Accuracy of the API content prediction should be further verified by analysing a larger sample size.

The T2 samples prepared with fine API particles resulted in a more uniform distribution of amlodipine in tablets (Figure S2), leading to higher average B values than all the samples included in the calibration. Therefore, a separate calibration is required to accurately determine the amlodipine content of the tablets with different API sizes. To address this issue, a particle size-based classification is proposed through pattern recognition neural networks (Mészáros et al., 2022).

The results underscore the importance of 100% quality control in order to ensure content uniformity and detect potential defects arising from inhomogeneities.
In traditional quality control, only a few tablets are tested from each batch, as a results these traditional methods face challenges in detecting outliers when the issue is limited to only a few samples. If out-of-spec drugs go undetected and remain in circulation, they present a significant risk to patients. In contrast, real-time and non-destructive analysis of the samples enables the examination of all products, facilitating the detection and removal of all outliers. Surface powder sticking in pharmaceutical mixing vessels poses a risk to the uniformity and quality of drug formulations. Towards the end of the homogenization process, the powder sticking to the vessel walls may dislodge either due to technician intervention or mechanical impact. Variations in material characteristics influence the degree of adhesion and cohesion. Consequently, dislodging the material stuck to the vessel walls could compromise the homogeneity of the final mixture,

leading to localized areas of uneven distribution that can affect the quality of the pharmaceutical product.

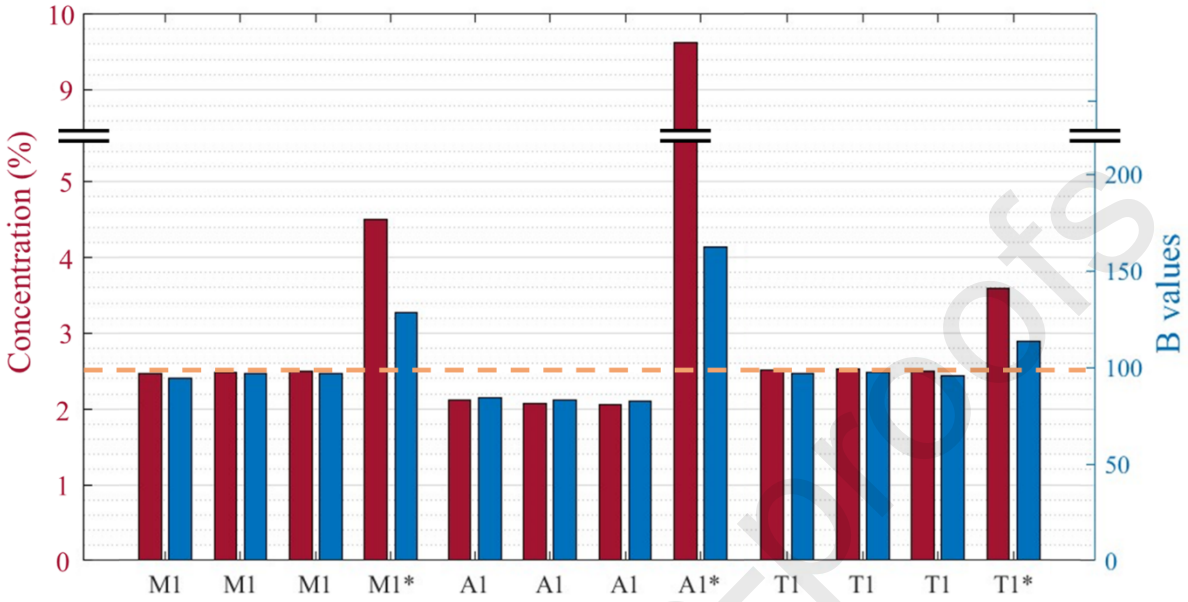

Figure 9: Concentration of tablets M1, A1, T1 from the original amlodipine mixture is shown in red, with the average B values of the tablets' UV images in blue. Tablets from the dislodged material are marked with an asterisk, and the target amlodipine concentration of 2.5% is indicated by a dashed line.

4. Conclusion

In this research, the adherence of pharmaceutical powder mixtures to stainless-steel surfaces was explored, with a particular emphasis on the sequence of component addition during the homogenization process. Amlodipine and microcrystalline cellulose were utilized as key components, and adherence was assessed using various analytical techniques. The results demonstrate that the quantity of the API adhering to the wall is influenced by the homogenization method. Substantial differences may occur when altering the sequence of component mixing and require careful consideration of the API particle size. The dislodged material from the vessel wall, either due to technician intervention or mechanical impact, may pose a risk to the uniformity and quality of drug formulations.

The distribution of the API on the stainless-steel surface was evaluated through UV imaging and Raman mapping. Machine vision-based chemical maps were obtained by combining the VIS and UV images of the samples, allowing for the analysis of a substantially larger area with high resolution, surpassing the capabilities of Raman mapping in terms of speed and area coverage. Image analysis of the UV images was suitable for differentiating between the tablets prepared with different-sized API. Colour analysis using UV imaging allowed for the identification of outliers in tablet content uniformity. UV imaging stands out as a fast, non-destructive tool, offering versatility and holding potential in formulation optimization. The integration of rapid digital imaging techniques, such as UV imaging, are promising for efficient quality control in pharmaceutical manufacturing. Nevertheless, further research is required to determine detection limits and reduce data acquisition time for enabling real-time analysis. The results highlight the importance of 100% quality control in order to ensure content uniformity and identify potential defects arising from inhomogeneities.

CRediT authorship contribution statement

Orsolya Péterfi: Investigation, Methodology, Formal analysis, Visualization, Writing – original draft. **Lilla Alexandra Mészáros:** Methodology, Software, Formal analysis. **Bence Szabó:** Investigation. **Máté Ficzere:** Formal analysis. **Emese Sipos:** Supervision, Writing – review & editing. **Attila Farkas:** Investigation, Formal analysis. **Dorián László Galata:** Conceptualization, Supervision, Writing – review & editing. **Zsombor Kristóf Nagy:** Supervision, Resources, Writing – review & editing.

Declaration of Competing Interest

The authors declare that they have no known competing financial interests or personal relationships that could have appeared to influence the work reported in this paper.

Acknowledgement

Project no. RRF-2.3.1-21-2022-00015 has been implemented with the support provided by the European Union. The research was supported by the Agency for Credits and Study Grants coordinated by the Romanian Ministry of National Education from the source of the research grant established through the Government Decision no. 118/2023, as well as the ÚNKP-23-3-I-BME-

23 and ÚNKP-23-3-I-BME-102 New National Excellence Program of the Ministry for Culture and Innovation from the source of the National, Research, Development and Innovation Fund. The project supported by the Doctoral Excellence Fellowship Programme (DCEP) is funded by the National Research Development and Innovation Fund of the Ministry of Culture and Innovation and the Budapest University of Technology and Economics, under a grant agreement with the National Research, Development and Innovation Office.

Bibliography

Abdel-Hamid, S., Alshihabi, F., Betz, G., 2011. Investigating the effect of particle size and shape on high speed tableting through radial die-wall pressure monitoring. Int. J. Pharm. 413, 29–35. https://doi.org/10.1016/j.ijpharm.2011.04.012

Abe, H., Otsuka, M., 2012. Effects of lubricant-mixing time on prolongation of dissolution time and its prediction by measuring near infrared spectra from tablets. Drug Dev. Ind. Pharm. 38, 412–419. https://doi.org/10.3109/03639045.2011.608679

Andrews, G.P., 2007. Advances in solid dosage form manufacturing technology. Philos. Trans. R. Soc. A Math. Phys. Eng. Sci. 365, 2935–2949. https://doi.org/10.1098/rsta.2007.0014

Beaudoin, S., Jaiswal, P., Harrison, A., Laster, J., Smith, K., Sweat, M., Thomas, M., 2015. Fundamental Forces in Particle Adhesion, in: Particle Adhesion and Removal. Wiley, pp. 1–79. https://doi.org/10.1002/9781118831571.ch1

Booth, S.W., Newton, J.M., 1987. Experimental investigation of adhesion between powders and surfaces. J. Pharm. Pharmacol. 39, 679–684. https://doi.org/10.1111/j.2042-7158.1987.tb06969.x

Bunker, M., Zhang, J., Blanchard, R., Roberts, C.J., 2011. Characterising the surface adhesive behavior of tablet tooling components by atomic force microscopy. Drug Dev. Ind. Pharm. 37, 875–885. https://doi.org/10.3109/03639045.2010.546402

Capece, M., 2019. The Role of Particle Surface Area and Adhesion Force in the Sticking Behavior of Pharmaceutical Powders. J. Pharm. Sci. 108, 3803–3813. https://doi.org/10.1016/j.xphs.2019.08.019

Chattoraj, S., Daugherity, P., McDermott, T., Olsofsky, A., Roth, W.J., Tobyn, M., 2018. Sticking and Picking in Pharmaceutical Tablet Compression: An IQ Consortium Review. J. Pharm. Sci. 107, 2267–2282. https://doi.org/10.1016/j.xphs.2018.04.029

Chu, K.R., Lee, E., Jeong, S.H., Park, E.S., 2012. Effect of particle size on the dissolution behaviors of poorly water-soluble drugs. Arch. Pharm. Res. 35, 1187–1195. https://doi.org/10.1007/s12272-012-0709-3

Frabetti, A.C.C., de Moraes, J.O., Jury, V., Boillereaux, L., Laurindo, J.B., 2021. Adhesion of Food on Surfaces: Theory, Measurements, and Main Trends to Reduce It Prior to Industrial Drying. Food Eng. Rev. 13, 884–901. https://doi.org/10.1007/s12393-021-09286-9

Galata, D.L., Mészáros, L.A., Kállai-Szabó, N., Szabó, E., Pataki, H., Marosi, G., Nagy, Z.K., 2021. Applications of machine vision in pharmaceutical technology: A review. Eur. J. Pharm. Sci. 159. https://doi.org/10.1016/j.ejps.2021.105717

Garg, V., Mallick, S.S., Garcia-Trinanes, P., Berry, R.J., 2018. An investigation into the flowability of fine powders used in pharmaceutical industries. Powder Technol. 336, 375–382. https://doi.org/10.1016/j.powtec.2018.06.014

Goodwin, D.J., van den Ban, S., Denham, M., Barylski, I., 2018. Real time release testing of tablet content and content uniformity. Int. J. Pharm. 537, 183–192. https://doi.org/10.1016/j.ijpharm.2017.12.011

Ibrahim, T.H., Burk, T.R., Etzler, F.M., Neuman, R.D., 2000. Direct adhesion measurements of pharmaceutical particles to gelatin capsule surfaces. J. Adhes. Sci. Technol. 14, 1225–1242. https://doi.org/10.1163/156856100742177

Jakubowska, E., Ciepluch, N., 2021. Blend segregation in tablets manufacturing and its effect on drug content uniformity—a review. Pharmaceutics 13. https://doi.org/10.3390/pharmaceutics13111909

Karner, S., Maier, M., Littringer, E., Urbanetz, N.A., 2014. Surface roughness effects on the tribo-charging and mixing homogeneity of adhesive mixtures used in dry powder inhalers. Powder Technol. 264, 544–549. https://doi.org/10.1016/j.powtec.2014.03.040

Katainen, J., Paajanen, M., Ahtola, E., Pore, V., Lahtinen, J., 2006. Adhesion as an interplay between particle size and surface roughness. J. Colloid Interface Sci. 304, 524–529. https://doi.org/10.1016/j.jcis.2006.09.015

Klukkert, M., Wu, J.X., Rantanen, J., Carstensen, J.M., Rades, T., Leopold, C.S., 2016. Multispectral UV imaging for fast and non-destructive quality control of chemical and physical tablet attributes. Eur. J. Pharm. Sci. 90, 85–95. https://doi.org/10.1016/j.ejps.2015.12.004

Mazel, V., Busignies, V., Diarra, H., Reiche, I., Tchoreloff, P., 2013. The surface layer of pharmaceutical compacts: The role of the punch surface and its impact on the mechanical properties of the compacts. Int. J. Pharm. 442, 42–48. https://doi.org/10.1016/j.ijpharm.2012.08.005

McDermott, T.S., Farrenkopf, J., Hlinak, A., Neilly, J.P., Sauer, D., 2011. A material sparing method for quantitatively measuring tablet sticking. Powder Technol. 212, 240–252. https://doi.org/10.1016/j.powtec.2011.05.023

Mészáros, L.A., Farkas, A., Madarász, L., Bicsár, R., Galata, D.L., Nagy, B., Nagy, Z.K., 2022. UV/VIS imaging-based PAT tool for drug particle size inspection in intact tablets supported by pattern recognition neural networks. Int. J. Pharm. 620. https://doi.org/10.1016/j.ijpharm.2022.121773

Mészáros, L.A., Galata, D.L., Madarász, L., Köte, Á., Csorba, K., Dávid, Á.Z., Domokos, A.,

Szabó, E., Nagy, B., Marosi, G., Farkas, A., Nagy, Z.K., 2020. Digital UV/VIS imaging: A rapid PAT tool for crushing strength, drug content and particle size distribution determination in tablets. Int. J. Pharm. 578, 119174. https://doi.org/10.1016/j.ijpharm.2020.119174

Mollereau, G., Mazel, V., Busignies, V., Tchoreloff, P., Mouveaux, F., Rivière, P., 2013. Image analysis quantification of sticking and picking events of pharmaceutical powders compressed on a rotary tablet press simulator. Pharm. Res. 30, 2303–2314. https://doi.org/10.1007/s11095-013-1074-8

Muselík, J., Franc, A., Doležel, P., Goněc, R., Krondlová, A., Lukášová, I., 2014. Influence of process parameters on content uniformity of a low dose active pharmaceutical ingredient in a tablet formulation according to GMP. Acta Pharm. 64, 355–367. https://doi.org/10.2478/acph-2014-0022

Neilly, J.P., Vogt, A.D., Dziki, W., 2009. Characterization of sticking residue on tablet punch faces by scanning electron microscopy and X-ray mapping. Microsc. Microanal. 15, 18–19. https://doi.org/10.1017/S1431927609097165

Novikova, A., Carstensen, J.M., Rades, T., Leopold, P.D.C.S., 2016. Multispectral UV imaging for surface analysis of MUPS tablets with special focus on the pellet distribution. Int. J. Pharm. 515, 374–383. https://doi.org/10.1016/j.ijpharm.2016.09.087

Novikova, A., Carstensen, J.M., Zeitler, J.A., Rades, T., Leopold, C.S., 2017. Multispectral UV Imaging for Determination of the Tablet Coating Thickness. J. Pharm. Sci. 106, 1560–1569. https://doi.org/10.1016/j.xphs.2017.02.016

Patel, R., Podczeck, F., 1996. Investigation of the effect of type and source of microcrystalline cellulose on capsule filling. Int. J. Pharm. 128, 123–127. https://doi.org/10.1016/0378-5173(95)04231-8

Paul, S., Taylor, L.J., Murphy, B., Krzyzaniak, J.F., Dawson, N., Mullarney, M.P., Meenan, P., Sun, C.C., 2020. Toward a Molecular Understanding of the Impact of Crystal Size and Shape on Punch Sticking. ACS Appl. Mater. Interfaces. https://doi.org/10.1021/acs.molpharmaceut.9b01185

Petean, P.G.C., Aguiar, M.L., 2015. Determining the adhesion force between particles and rough surfaces. Powder Technol. 274, 67–76. https://doi.org/10.1016/j.powtec.2014.12.047

Podczeck, F., 2004. Powder, Granule and Pelett Properties for Filling of Two-Piece Hard Capsules, in: Podczeck, F., Jones, B.E. (Eds.), Pharmaceutical Capsules. Pharmaceutical Press, London, pp. 101–117.

Podczeck, F., 1999. Investigations into the reduction of powder adhesion to stainless steel surfaces by surface modification to aid capsule filling. Int. J. Pharm. 178, 93–100. https://doi.org/10.1016/S0378-5173(98)00363-9

Preedy, E.C., Perni, S., Prokopovich, P., 2015. Adhesion Phenomena in Pharmaceutical Products and Applications of AFM. Prog. Adhes. Adhes. 2, 221–243.

https://doi.org/10.1002/9781119162346.ch5

Rhodes, E., Everett, J.R., Whiteside, P., Kraus, D., Cram, M., Dawson, N., 2022. Assessment of Prediction Models for Punch Sticking in Tablet Formulations. Br. J. Pharm. 4–5. https://doi.org/10.5920/bjpharm.1118

Salazar-Banda, G.R., Felicetti, M.A., Gonçalves, J.A.S., Coury, J.R., Aguiar, M.L., 2007. Determination of the adhesion force between particles and a flat surface, using the centrifuge technique. Powder Technol. 173, 107–117. https://doi.org/10.1016/j.powtec.2006.12.011

Simmons, D.M., 2019. Punch sticking: Factors and solutions. Chem. Eng. Pharm. Ind. 227–243. https://doi.org/10.1002/9781119600800.ch60

Simmons, D.M., Gierer, D.S., 2012. A material sparing test to predict punch sticking during formulation development. Drug Dev. Ind. Pharm. 38, 1054–1060. https://doi.org/10.3109/03639045.2011.637933

Stauffer, F., Vanhoorne, V., Pilcer, G., Chavez, P.F., Rome, S., Schubert, M.A., Aerts, L., De Beer, T., 2018. Raw material variability of an active pharmaceutical ingredient and its relevance for processability in secondary continuous pharmaceutical manufacturing. Eur. J. Pharm. Biopharm. 127, 92–103. https://doi.org/10.1016/j.ejpb.2018.02.017

Stevenson, C., Monroe, J., Vazquez, J.M., Jones, O., Zhang, R., Main, E., Upton, J., Cheah, W., Park, S., Nobbe, B., Sura, I., Roberts, T., Vogt, A., Capece, M., Ketterhagen, W., Beaudoin, S., 2023. The effects of humidity on the adhesion of pharmaceutical excipients to steel surfaces. Powder Technol. 119160. https://doi.org/10.1016/j.powtec.2023.119160

Takeuchi, Y., Murase, Y., Tahara, K., Takeuchi, H., 2020. Impact of surface roughness of pre-treated punches and powder properties on prevention of sticking during pharmaceutical tableting. J. Drug Deliv. Sci. Technol. 60, 101999. https://doi.org/10.1016/j.jddst.2020.101999

Tan, S.B., Newton, J.M., 1990. Influence of capsule dosator wall texture and powder properties on the angle of wall friction and powder-wall adhesion. Int. J. Pharm. 64, 227–234. https://doi.org/10.1016/0378-5173(90)90273-7

Thomas, M.C., Beaudoin, S.P., 2015. An enhanced centrifuge-based approach to powder characterization: Particle size and Hamaker constant determination. Powder Technol. 286, 412–419. https://doi.org/10.1016/j.powtec.2015.08.010

Tsosie, H., Thomas, J., Strong, J., Zavaliangos, A., 2017. Scanning Electron Microscope Observations of Powder Sticking on Punches during a Limited Number (N < 5) of Compactions of Acetylsalicylic Acid. Pharm. Res. 34, 2012–2024. https://doi.org/10.1007/s11095-017-2186-3

Uzunović, A., Vranić, E., 2007. Effect of magnesium stearate concentration on dissolution properties of ranitidine hydrochloride coated tablets. Bosn. J. Basic Med. Sci. 7, 279–283. https://doi.org/10.17305/bjbms.2007.3060

Waknis, V., Chu, E., Schlam, R., Sidorenko, A., Badawy, S., Yin, S., Narang, A.S., 2014. Molecular basis of crystal morphology-dependent adhesion behavior of mefenamic acid during tableting. Pharm. Res. 31, 160–172. https://doi.org/10.1007/s11095-013-1149-6

Wang, Z., Shah, U. V., Olusanmi, D., Narang, A.S., Hussain, M.A., Gamble, J.F., Tobyn, M.J., Heng, J.Y.Y., 2015. Measuring the sticking of mefenamic acid powders on stainless steel surface. Int. J. Pharm. 496, 407–413. https://doi.org/10.1016/j.ijpharm.2015.09.067

Wu, J.X., Rehder, S., Berg, F. van den, Amigo, J.M., Carstensen, J.M., Rades, T., Leopold, C.S., Rantanen, J., 2014. Chemical imaging and solid state analysis at compact surfaces using UV imaging. Int. J. Pharm. 477, 527–535. https://doi.org/10.1016/j.ijpharm.2014.10.064

Zakhvatayeva, A., Hare, C., Wu, C.Y., 2019. Size-induced segregation during die filling. Int. J. Pharm. X 1. https://doi.org/10.1016/j.ijpx.2019.100032

Zimon, A.D., 1982. Fundamental Concepts of Particle Adhesion, in: Zimon, A.D. (Ed.), Adhesion of Dust and Powder. Plenum Publishing Corporation, Moscow, pp. 1–9.

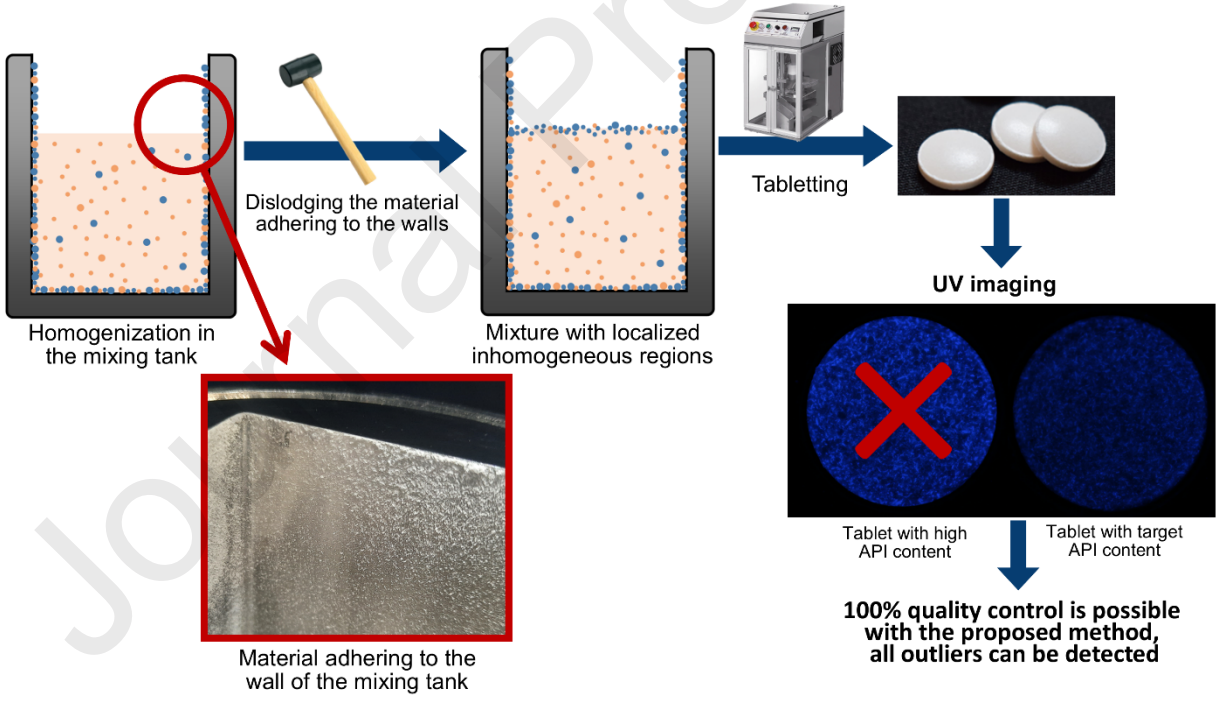

Declaration of interests

☒ The authors declare that they have no known competing financial interests or personal relationships that could have appeared to influence the work reported in this paper.

☐ The authors declare the following financial interests/personal relationships which may be considered as potential competing interests: